Wave Energy Resources at the Test Site in Keelung, Taiwan

Tzang, S.Y. [#1], **Chen C.C.** [#2], **Chen, Y.L.** [*3], **Chen, H.Z.** [#4], **Chen, J.H.** [##5]

[#] *Department of Harbor & River Engineering,* [##] *Department of Systems Engineering and Naval Architecture*
National Taiwan Ocean University, 2nd Pei-Ning Rd. Keelung, 202, Taiwan, ROC
[1]*sytzang@ntou.edu.tw*
[2]jimmie243@gmail.com
[4]10652017@mail.ntou.edu.tw
[5]*b0105@ntou.edu.tw*
[*]*Minesto Taiwan Ltd.*
24F, No. 333 Keelung Rd. Sec. 1, Taipei 11012, Taiwan, ROC
[3]yunglung.chen@minesto.com

***Abstract*— Wave energy comprises the most abundant resource among the marine renewable energy in the world. Offshore Taiwan, it is also one of the prior marine energy resources and higher nearshore wave energy resources are located in the north-eastern (NE) waters. Thus, to facilitate the development of the wave energy conversion technology, a permitted field-test site offshore Keelung was established in 2011. The associated wave energy resources had been collected with a data buoy being deployed at the offshore boundary of the test site since 2012. This study presents the analysed results from May 2012 to May 2015. Typical joint probability distributions between wave height H and period T in four seasons and monsoon seasons were first shown. The calculated monthly variations of averaged wave energy resources were also presented. The results clearly illustrate that in the NE Monsoon season (Oct. to next March) waves are higher and longer resulting in average wave power density to be about 15 kW/m with directions from ENE to NE.**

***Keywords*— wave energy, test site, wave buoy, north eastern Taiwan, monsoon**

I. INTRODUCTION

Keelung is located in the northeast Taiwan facing the Pacific Ocean (Fig. 1). In the winter monsoon season, the dominant wind direction is north-eastern due to high pressure atmospheric systems from above Mainland China. Around coastal waters of Taiwan, the monsoon wind fields also result in larger wave climates along the northeast coastal waters ([1, 2]). For about six months in monsoon season, i.e. October to March of next year, the average wave power could generally range from 10-15 kW/m ([3, 4]).

Thus, a field test site for wave energy converters (WECs) was selected and successfully applied for test permission in coastal waters offshore Keelung. Figure 1 illustrates that at the offshore boundary 500 m offshore in the permitted WEC test site, wave data had been collected continuously with a sampling rate of 2Hz by an Oce/Met Data Buoy at a depth of about 40 m since May, 2012. Hourly data including wave heights, periods and directions were simultaneously transmitted through wireless communication of GPRS to a nearby land-based receiving station.

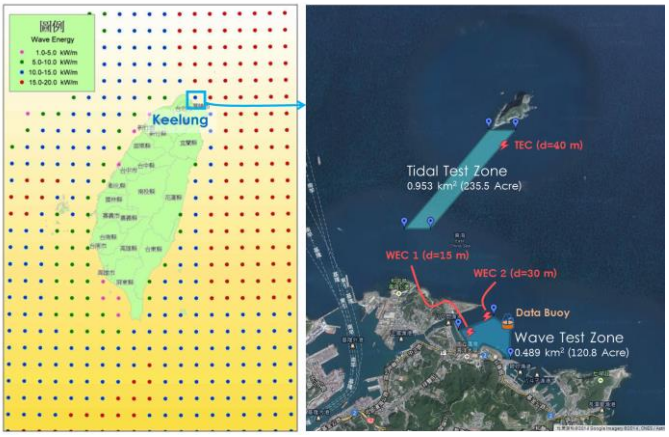

Fig. 1 The wave and tidal current energy test site offshore Keelung

II. DATA PROCESSNG & FORMULATION

The processing of the measured wave data for joint probability consists of significant wave height H_s ranging from 0-7 m with an interval of 0.5 m and peak period T_p ranging from 0-14 s with an interval of 1 s. Equal lines of probability between 3-7 % and wave power between 5-80 kW/m were also drawn on the results. For deriving the statistics of exploitable wave power, values larger than 80 kW/m were intentionally deleted in present study. Those waves are of heights larger than 4.5 m and periods longer than 8 s mostly occurring during summer in extreme typhoon events around offshore Taiwan ([3]). In a few events in winter monsoon seasons, waves of heights larger than 4 m and periods longer than 10 s could result in power more than 80 kW/m along the NE coastal waters. The wave power at a finite depth h is generally formulated as follows (e.g. [5])

$$P(T_e,h)=\left(\frac{\rho g}{16}\right)C_g(T_e,h)H_s^2 \tag{1}$$

By taking water density ρ =1025 kg/m^3 and gravitational acceleration g=9.81 m/s^2, Eq. (1) can be rewritten as

$$P\approx 0.628C_g(T_e,h)H_s^2 \quad (unit:\ kW/m) \tag{2}$$

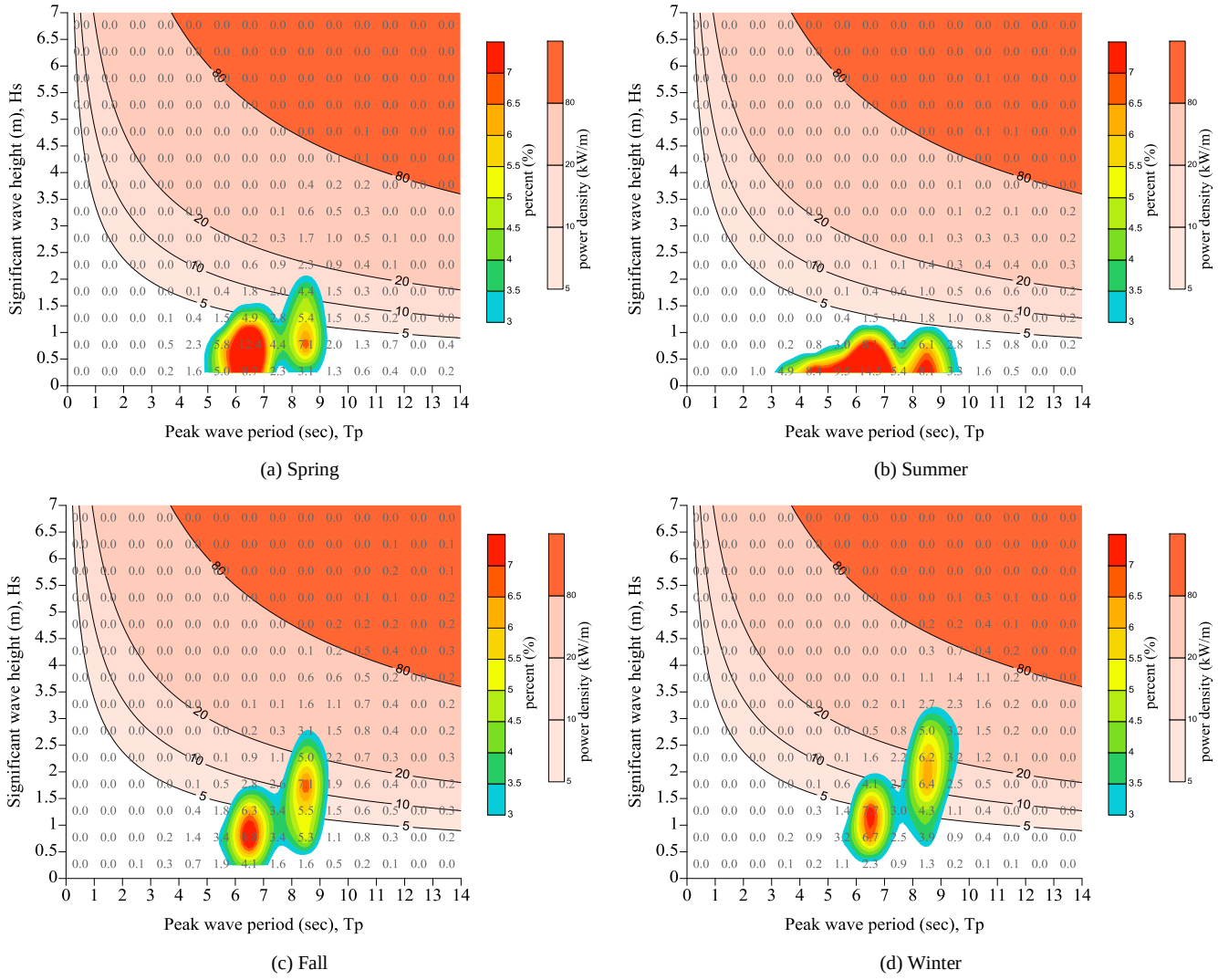

Fig. 2 Joint probability distributions of wave heights and periods for four seasons

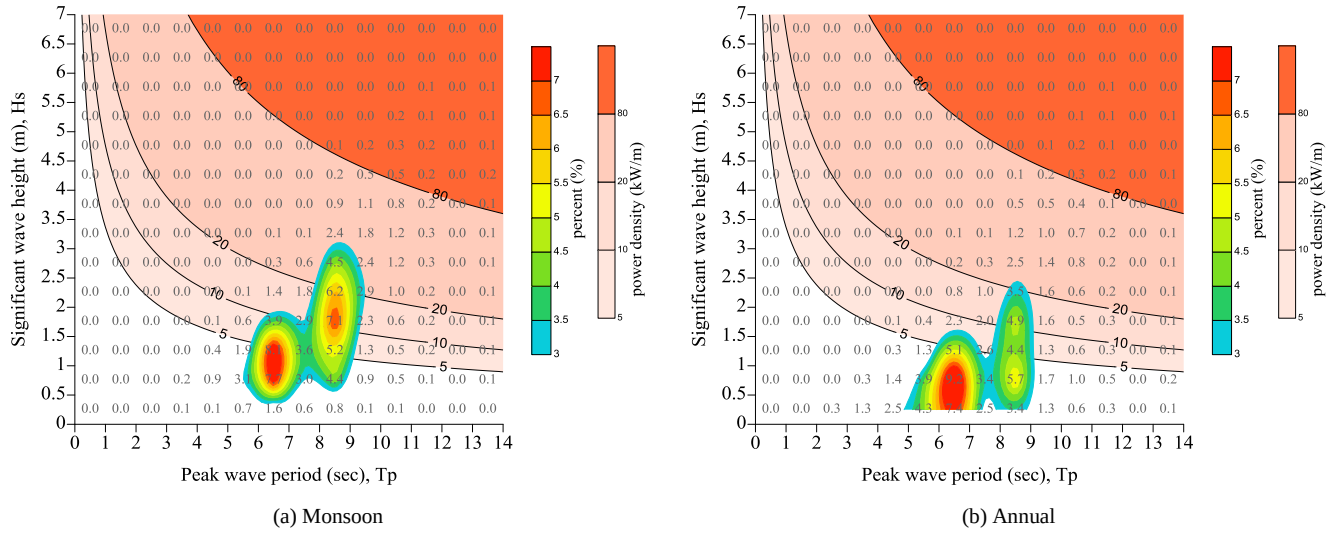

Fig. 3 Joint probability distributions of wave heights and periods for (a) Monsoon seasons and (b) Yearly average

where C_g is the group velocity and T_e is the wave energy period ([6]) and both are commonly adopted as

$$C_g(T_e,h)=\frac{gT_e}{4\pi}\tanh(kh)\left[1+\frac{2kh}{\sinh(2kh)}\right] \quad (3)$$

$$T_e=0.9T_p \quad (4)$$

III. Wave Resources Characteristics

The 3-year average wave statistics were derived and displayed in four seasons, monsoon season and 3-year average. The Winter season in Taiwan are commonly defined as months from December to February of next year and Spring, Summer and Fall are defined for following every three months.

A. Joint Probability Diagram

Fig. 2 displays the joint probability of wave heights and periods for four seasons. The distribution patterns typically illustrate double-peak occurrence ratios larger than 3%. In Spring, the peak ratios occurred in periods of 5-7.5 s and 7.5-9 s and in heights of 0-1.5 m and 0.25-2 m, respectively. In Summer, the peak ratios occurred in periods of 3-7.5 s and 7.5-10 s and in heights of similarly 0-1 m, respectively. In Fall, the peak ratios occurred in periods of 5.5-7.5 s and 7.5-9 s and in heights of 0.25-1.5 m and 0.5-2.75 m, respectively. In Winter, the peak ratios occurred in periods of 5.5-7.5 s and 7.5-9.5 s and in heights of 0.25-2 m and 0.5-3.25 m, respectively. Most of the occurrence ratios higher than 7% are located in peaks of shorter periods. The ranges of wave periods of the two peak ratios were quite similar in all four seasons. But wave heights are clearly seen to become smaller in Summer and start to increase through Fall and Winter and again to decrease from Spring. The slightly longer periods in Summer were mainly due to typhoon swells.

Fig. 3 further displays the joint probability distributions in monsoon season and in the whole year. As mentioned above, the monsoon season begins in later Fall (October) and ends in later Spring (March) of next year. It is clearly seen that the peak-ratio ranges are quite similar to those in Winter with slightly higher occurrence ratios in longer periods. The peak-ratios of yearly average are quite similar in periods to those in Spring but with slightly higher heights.

B. Rose Maps of Wave Heights

The rose maps in four seasons and monsoon season are clearly seen in

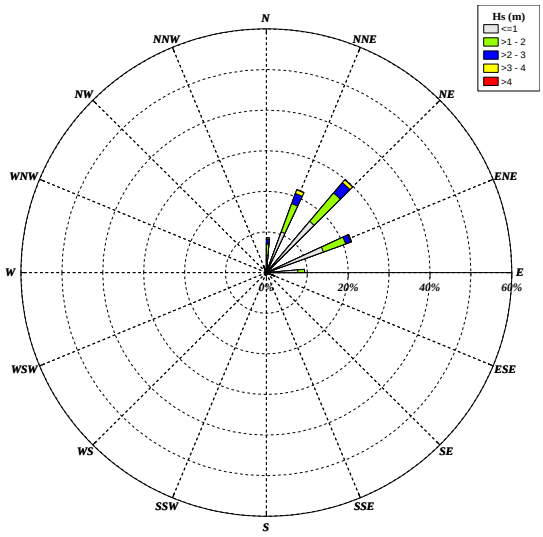

(a) Spring

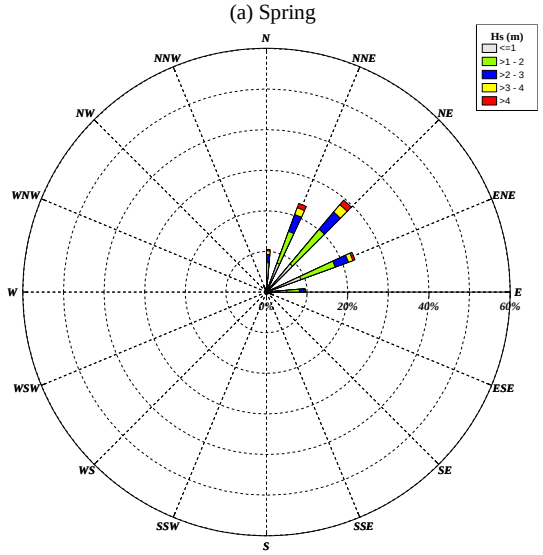

(c) Fall

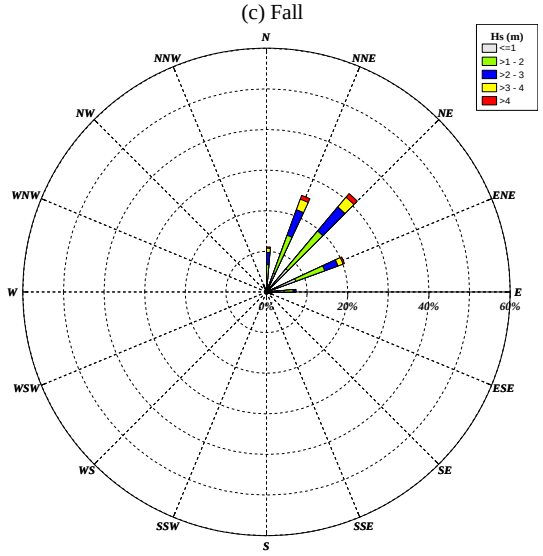

(e) Monsoon

Fig. 4 that the highest probability all occurred in NE direction and slightly decrease in NNE and ENE directions. The three directions occurred in the four seasons from Spring

with total probabilities of 73.9%, 67.1 %, 75.0% and 77.6%, respectively. The results for monsoon season are quite similar to those in Winter with a total probability of 77.3% for the same three directions. The results imply that the waves coming into the Keelung test site are mainly centred in the NE direction with quite narrow band in directions.

C. Monthly Distribution of Average Power Density

Fig. 5 display the calculated average monthly power density from December to next November in each investigated year by adopting Eqs. (1)~(4). We immediately notice in Figure 5a that the power density typically distributes in a U shape, i.e. lower than 10 kW/m in months from April to August and higher in the other months. In those months exceeding 10 kW/m, the average power density could even be higher than 20 kW/m. Figure 5b further illustrates the occurrence ratios of power in months exceeding 10 kW/m generally range from 30% to 60 %. In particular, the extreme power density exceeding 80 kW/m is noticed to occur in two peak periods, one from August to October with values up to about 15% and the other from December to February with values up to 8%. It confirms that waves by both typhoons and strong monsoon winds could result in power exceeding 80 kW/m but the occurrence ratios are much higher in typhoon seasons, general from May to October.

Thus by deleting the data with power density exceeding 80 kW/m, Fig. 6 clearly demonstrates the same U-shape monthly distributions in each interrogated year. It is again noted that the extreme high average power exceeding 20 kW/m in Fig. 5(a) are mainly due to waves with power exceeding 80 kW/m. However in those months, the percentages of waves with power exceeding 10 kW/m seem to remain similar by comparing Fig. 6(b) with Fig. 5(b). As a result from Fig. 6, the 6 months from October to next March could have average monthly power density higher than 10 kW/m and with more than 30% of the occurrence probability.

As a result, the statistics give that values of the average power yearly and in monsoon without deleting those exceeding 80 kW/m are 12.35 &18.51 kW/m, respectively. Even with deleting those exceeding 80 kW/m, the values decrease slightly to be 9.9 & 15.0 kW/m, respectively. Therefore, the deletions of data with power more than 80 kW/m had reduced the yearly average power slightly lower than 10 kW/m, the bottom-line of economic exploitability in Taiwan. But the values become as high as 15.02 kW/m in monsoon for at least 6 months, which is about 1.5 time higher.

D. Rose Maps of Power Density

Fig. 7 illustrate similar trends of quite narrow bands of spreading direction from NNE to ENE of the power to those of waves in the test site. In particular, the power density exceeding 10 kW/m could amount to more than 20% in both ENE and NE directions in Spring, Fall and Winter seasons. In the monsoon season, the distribution patterns are quite similar to those of Winter season. The focus of spreading directions of waves and power density suggest the dominant direction references for any WEC to adopt for its deployment engineering.

E. Power Scattering Diagram

Based on Fig. 3, we further derive the scatter diagram, or the joint probability diagram, for yearly average of accumulated wave power, as shown in Fig. 8. It is further noted that the top 7 values of accumulated power are all higher than 8,700 kW/m and are located within wave heights of from 1.75 m to 3.25 m and periods of from 8.5 to 9.5 s.

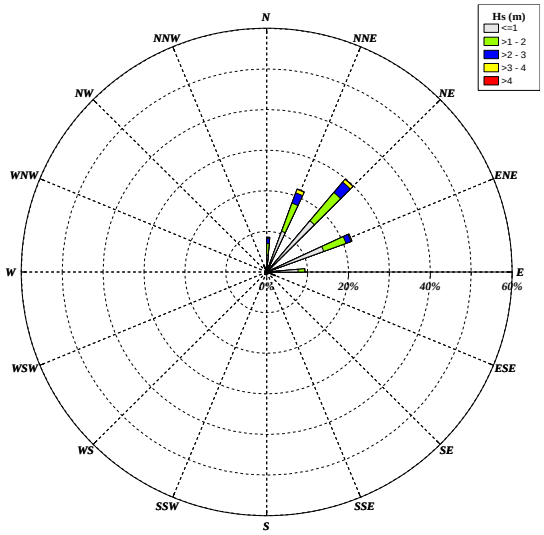

(a) Spring

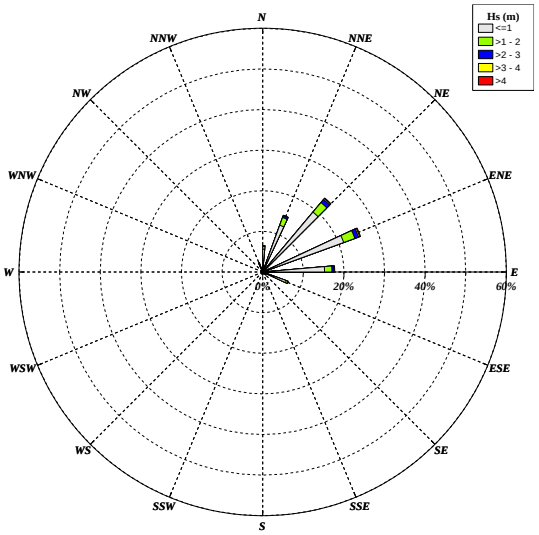

(b) Summer

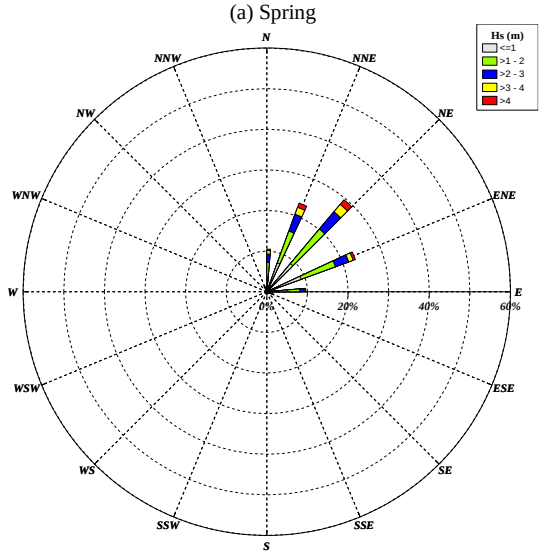

(c) Fall

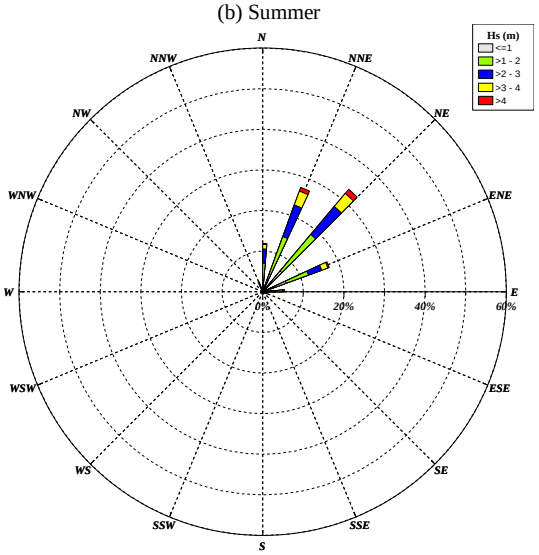

(d) Winter

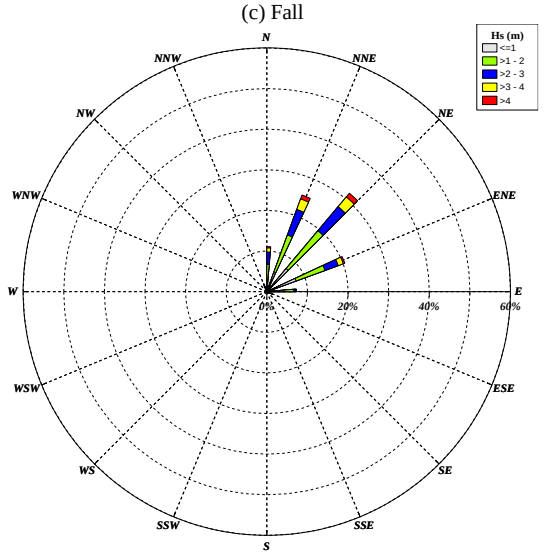

(e) Monsoon

Fig. 4 Rose maps of wave heights in four seasons and monsoon season

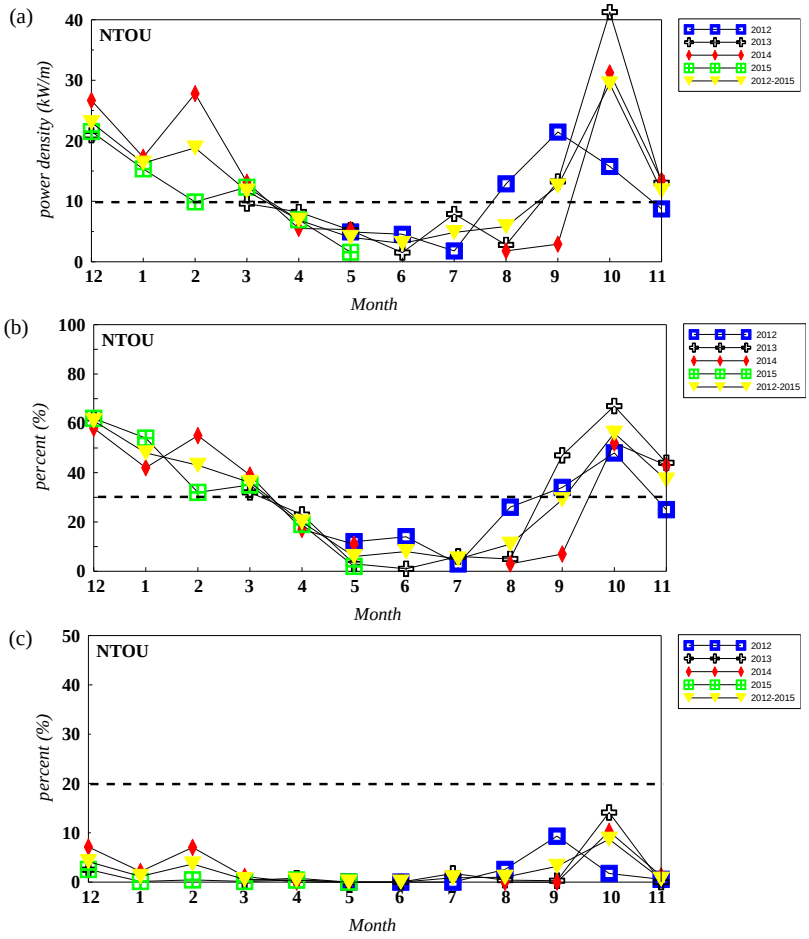

Fig. 5 (a) Average monthly and (b) occurrence probability of wave powers over 10 kW/m with (c) occurrence probability of wave powers over 80 kW/m

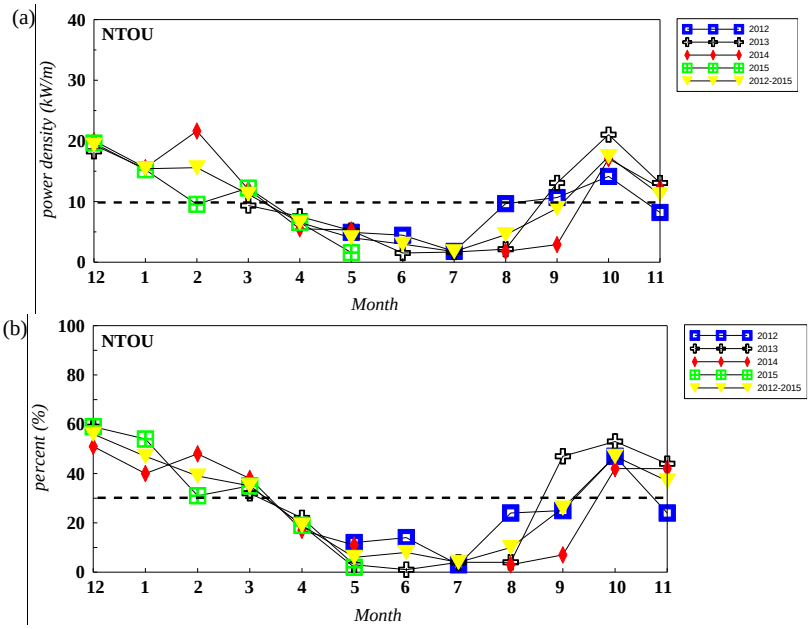

Fig. 6 (a) Average monthly wave powers and (b) occurrence probability of wave powers over 10 kW/m which were removed the values over 80 kW/m

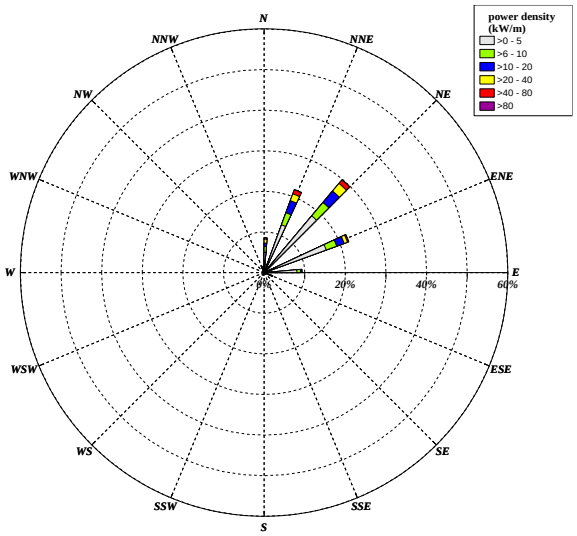

(a) Spring

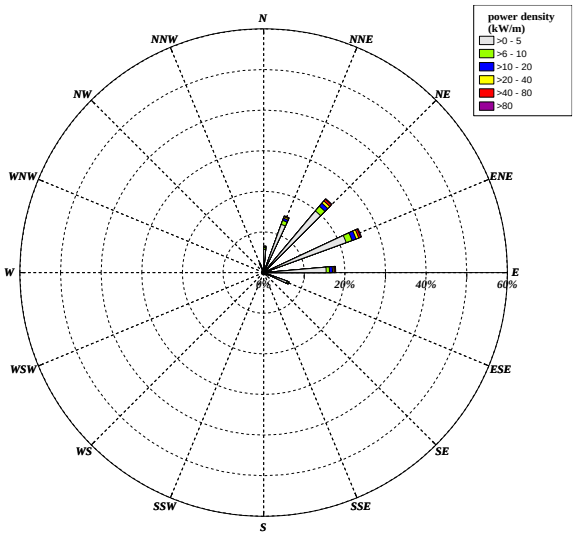

(b) Summer

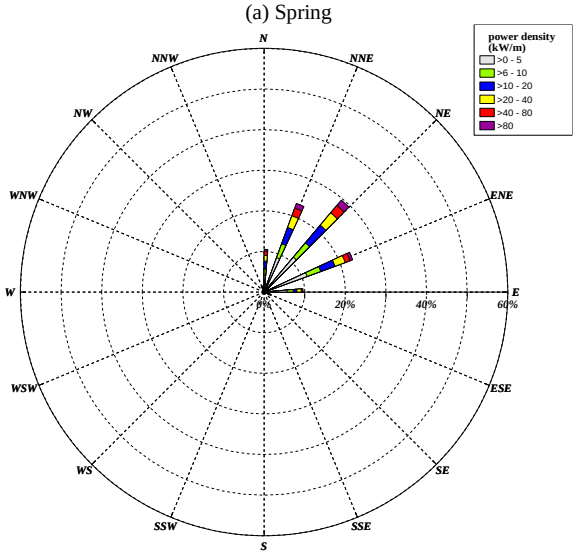

(c) Fall

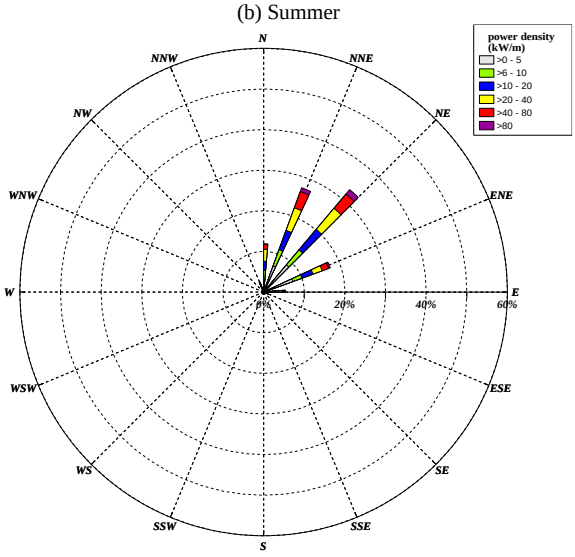

(d) Winter

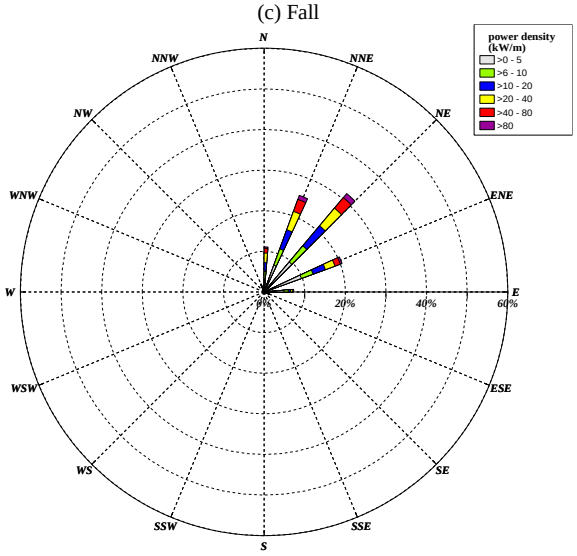

(e) Monsoon

Fig. 7 Rose maps of wave powers in four seasons and monsoon season

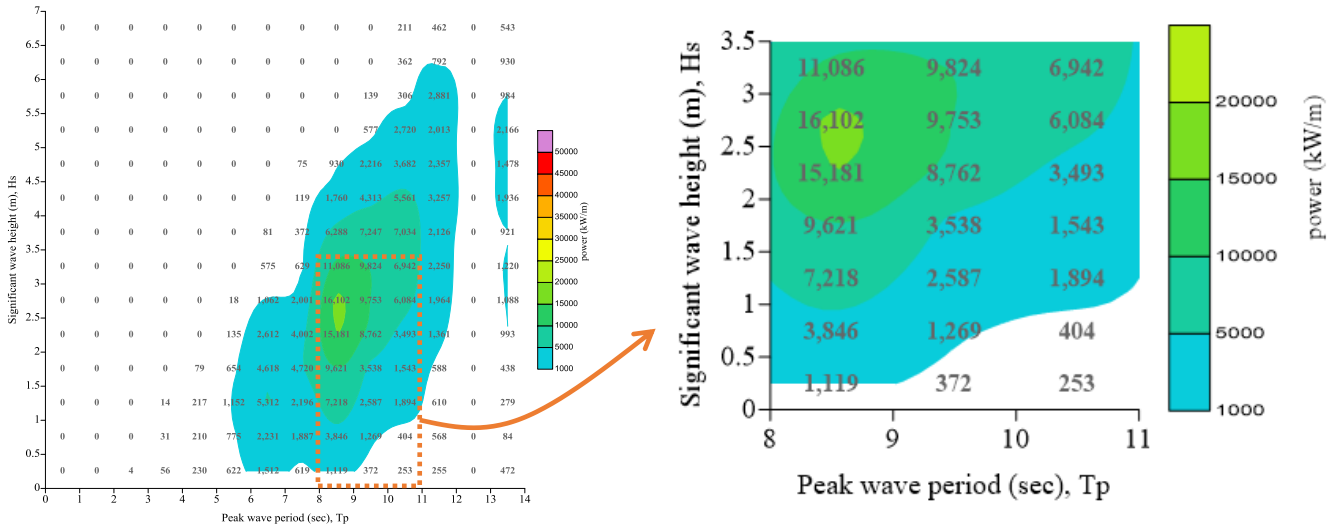

Fig. 8 Power scattering diagram for yearly average of accumulated wave power and the close-up of peak power zones

That is, the 7 highest values of accumulated power are all less than 80 kW/m and generated mainly by monsoon waves, rather by extreme typhoon waves. In addition, the two-peak distributions at periods of 6.5 & 8.5 s for wave resources have resulted in only one-peak distribution at periods of 8.5 s for accumulated wave power. The scatter diagram of wave power resources could further provide developers to derive their own power maps for test planning in present test site.

IV. Conclusions

For establishing database for wave energy in the selected test site for wave energy converters offshore Keelung, Taiwan a data buoy was deployed at a depth of 40 m on the offshore boundary since May, 2012. The in-site measurements of waves since May, 2012 to May, 2015 were first analyzed for wave and wave energy characteristics. The joint probabilities of wave heights and periods give similarly double-peak distributions at periods of 6.5 & 8.5 s in four seasons while the patterns of Monsoon season, i.e. October to next March, are much similar to those of the Winter season (December to next February). The waves in four seasons and monsoon season generally direct from ENE to NEN while in monsoon season the direction focus even around ENE to NE. The derived wave power have shown a typical U-shaped averaged monthly distribution with lower wave power around summer months from April to September and higher in the rest 6 Monsoon months of a year. Even by deleting the power exceeding 80 kW/m, generally associated with typhoon events, the averages annually and in monsoon are about 9.9 and 15.0 kW/m, respectively. The wave power in a year spreads also from ENE to NEN, especially around NE directions with more than 30% in each month of occurrence, wave powers could exceed the economically feasible 10 kW/m. As a result, the power scattering diagram have illustrated that the peak accumulated power occur with values less than 80 kW/m and at a period of about 8.5 s for waves with heights of 1.75 to 3.25 m. For the test site offshore Keelung, waves and wave power are quite similarly incident within narrow-banded directions from ENE to NE.

Acknowledgment

The authors are grateful for the financial support of National Science Council of Taiwan under the contract No. NSC 101-3113-P-019-002 & NSC 102-3113-P-019-002.

References

[1] Hsu P. H. and Yen C. W. (2007): Prospects for marine energy development in Taiwan. Physical bimonthly, vol.29, p718-726 (in Chinese)

[2] Tsai C. P., Hwang C. H., Hwa C., Cheng H. Y. (2012), "Study on the wave climate variation to the renewable wave energy assessment", Renewable energy, Vol.38 No.1, p.50-61.

[3] Tzang, S.-Y., Wang, C.-C., Chen, D.-W., Yang, J.-Z., Hsieh, C.-M., Chen, J.-H., 2012. "Wave Energy Resources on Coastal Waters of Northeast Taiwan," *The 4th International Conference on Ocean Energy*, Dublin, Ireland, Section. 2-1 No.2.

[4] Chiu F. C., Huang W.Y., Tiao W. C. (2013), "The spatial and temporal characteristics of the wave energy resources around Taiwan", Renewable energy, vol.52, p.218-221.

[5] Tucker M. J. and Pitt E. G. (2001): Waves in ocean engineering, Elsevier ocean engineering book series vol.5, Elsevier, Amsterdam, p.521.

[6] Cornett, A (2006): Inventory of Canada's Marine renewable Energy Sources, Tech. Rep. CHC-TR-041, Canadian Hydraulics Centre.